



A Journal of the Gesellschaft Deutscher Chemiker

Angewandte Chemie

GDCh

International Edition

www.angewandte.org

Accepted Article

Title: Conformationally Programmable Chiral Foldamers with Compact and Extended Domains Controlled by Monomer Structure

Authors: Peter Clarke Knipe and Zachariah Lockhart

This manuscript has been accepted after peer review and appears as an Accepted Article online prior to editing, proofing, and formal publication of the final Version of Record (VoR). This work is currently citable by using the Digital Object Identifier (DOI) given below. The VoR will be published online in Early View as soon as possible and may be different to this Accepted Article as a result of editing. Readers should obtain the VoR from the journal website shown below when it is published to ensure accuracy of information. The authors are responsible for the content of this Accepted Article.

To be cited as: *Angew. Chem. Int. Ed.* 10.1002/anie.201802822
Angew. Chem. 10.1002/ange.201802822

Link to VoR: <http://dx.doi.org/10.1002/anie.201802822>
<http://dx.doi.org/10.1002/ange.201802822>

COMMUNICATION

Conformationally Programmable Chiral Foldamers with Compact and Extended Domains Controlled by Monomer Structure

Zachariah Lockhart and Peter C. Knipe*

Abstract: Foldamers are an important class of abiotic macromolecules, with potential therapeutic applications in the disruption of protein-protein interactions. The majority adopt a single conformational motif such as a helix. Here we introduce a new class of foldamer where the choice of heterocycle within each monomer – coupled with a strong conformation-determining dipole repulsion effect – allows both helical and extended conformations to be selected. Combining these monomers into hetero-oligomers enables highly controlled exploration of conformational space and projection of side-chains along multiple vectors. The foldamers were rapidly constructed via an iterative deprotection-cross-coupling sequence, and their solid- and solution-phase conformations were analysed by X-ray crystallography and NMR and CD spectroscopy. These molecules may find applications in protein surface recognition where the interface does not involve canonical peptide secondary structures.

Nature's oligomers carry out many of the biological functions necessary to sustain life and carry genetic information. The majority of proteins adopt a structure determined entirely by the primary sequence of amino acids,^[1] containing α -helical, β -strand/sheet and loop domains combined in a tertiary fold. A key determinant of protein conformation is the secondary structural propensity (SSP) of the constituent amino acids, i.e. the structure of each creates a thermodynamic driving force for it to occupy a particular secondary structural environment (Figure 1A).^[2]

For decades chemists have sought to mimic the structural and functional diversity of biopolymers using synthetic oligomers, a field now known as foldamer chemistry.^[3] As well as catalytic^[4] and signalling applications,^[5] foldamers have enjoyed success when applied to problems in chemical biology^[3b] such as modulating protein-protein interactions (PPIs).^[6] One approach to controlling global conformation is to exploit non-covalent interactions between adjacent monomers. Gong^[7] and Huc^[8] have used hydrogen bonding to control curvature in aryl amide foldamers, while Aggarwal^[9] employed the *syn*-pentane interaction as a controlling force in simple hydrocarbon foldamers.^[10] Lehn pioneered the use of dipolar repulsion as a controlling element in foldamer design, and exploited aromatic heterocycles as 'shape codons'^[11] for helix formation due to their well-defined bond angles and strong dipoles.^[12] Dipole repulsion between carbonyl groups has also been explored;^[13] Clayden used this effect as a stereochemical relay to achieve remote (1,23)-asymmetric induction in an oligoxanthene foldamer.^[14] As a result of these and other approaches, chemists are now able to

synthesize foldamers that reliably adopt conformations analogous to protein secondary structures.^[15]

Efforts have been made to go beyond forming simple secondary structural motifs. Super-secondary helical foldamer bundles and beta helices have been reported,^[16] and recently Horne has used β -, *N*-methyl- and other modified amino acids to stabilize a natural zinc finger domain.^[17] Similarly, Kirshenbaum has used the presence of peptoids, in combination with cation- π interactions, to form stable β -loop-PPII helix tertiary peptidomimetics.^[18] The task of combining entirely unnatural secondary domains in a single foldamer capable of mimicking tertiary structure (called 'tylogomers' by Moore^[3c]) remains a central challenge, although Huc recently disclosed a remarkable helix-sheet-helix tertiary foldamer.^[19]

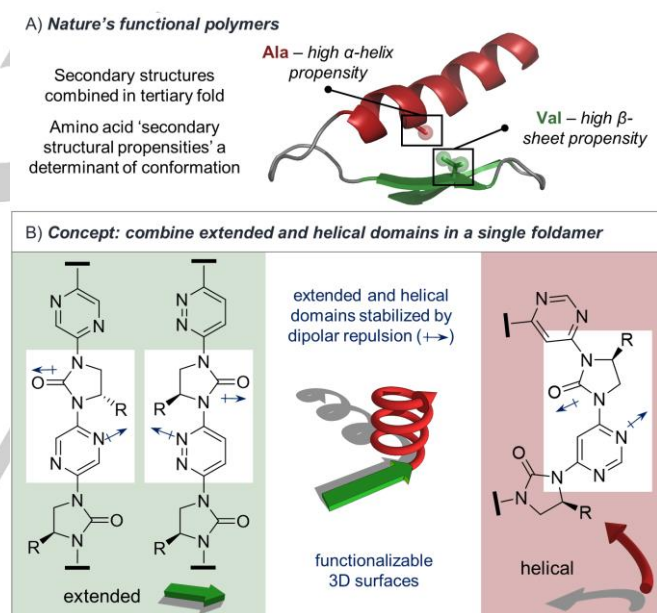


Figure 1. A) Nature's control of tertiary structure with amino acid secondary structural propensities (SSPs) as a determinant. Shown is a truncate of ephrin A2 receptor protein kinase (PDB: 5NKB). Side-chains A664 and V681 are highlighted. B) Left: aryl-imidazolidin-2-one monomers preferring an extended (linear) conformation due to dipolar repulsion. Selected dipoles are indicated. Right: pyrimidine-imidazolidin-2-one monomers preferring a helical conformation. Centre: representation of multi-domain foldamer structures.

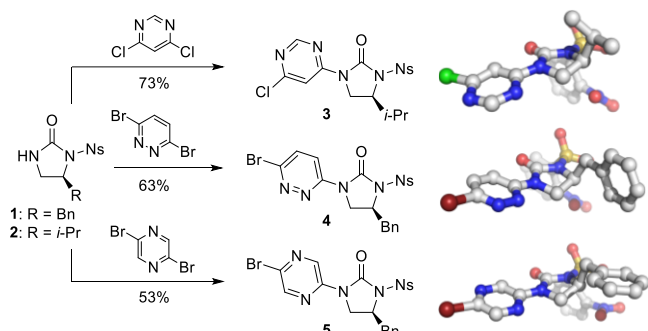
Inspired by Thompson and Hamilton's use of dipole repulsion to stabilize extended foldamer β -strand mimetics,^[15d,e] here we report the rational design of a range of monomers with different innate folding preferences, analogous to amino acid SSPs.^[20] These allow the selective formation of helical or extended domains within a single foldamer, formed by an iterative cross-coupling strategy. We theorized that use of three isomeric aromatic linkers – pyrazine, pyridazine, and pyrimidine – would lead to different conformational preferences in aryl-linked imidazolidine-2-one oligomers, as determined by dipolar repulsion between the urea carbonyl groups and adjacent arene

[*] Z. Lockhart, Dr. P. C. Knipe
School of Chemistry and Chemical Engineering, Queen's University Belfast, David Keir Building, Belfast, BT9 5AG (UK)
E-mail: p.knipe@qub.ac.uk
Homepage: www.knipechem.co.uk

Supporting information for this article is given via a link at the end of the document.

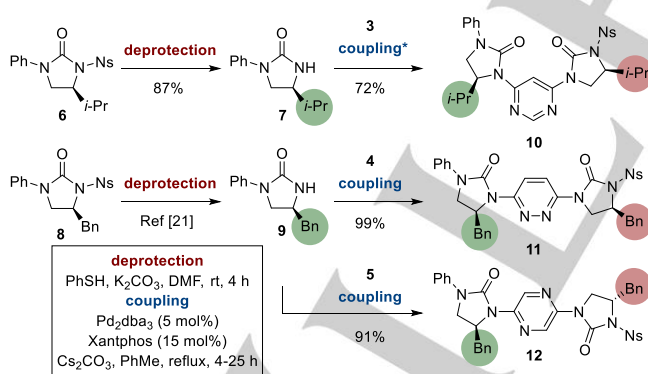
COMMUNICATION

nitrogen lone pairs (Figure 1B). The effect would be that the pyrazine and pyridazine linkers would stabilize extended conformations, while the pyrimidine linker would form curved or helical structures.^[11,12]



Scheme 1. Synthesis of monomers **3-5** via Buchwald-Hartwig cross-coupling. Single crystal X-ray structures show all compounds adopting the conformation in which dipoles are opposed. Coupling conditions: aryl dihalide (5 eq.), Pd₂dba₃ (5 mol%), Xantphos (15 mol%), Cs₂CO₃, PhMe, reflux, 30 min – 4 h. Bn = benzyl, dba = dibenzylideneacetone, Ns = 2-nitrobenzenesulfonyl, Xantphos = 4,5-bis(diphenylphosphino)-9,9-dimethylxanthene.

Our iterative approach to the foldamers required the synthesis of pyrimidine (**3**), pyridazine (**4**) and pyrazine (**5**) monomers, which was achieved from common intermediates **1** and **2** (Scheme 1).^[21] Buchwald-Hartwig coupling of **2** with 4,6-dichloropyrimidine, and of **1** with 3,6-dibromopyridazine and 2,5-dibromopyrazine, afforded monomers **3**, **4** and **5** in 73%, 63% and 53% yields respectively. The conformations of monomers **3-5** were examined by single crystal X-ray diffraction.^[22] In all cases the urea carbonyl is oriented *anti* to the *ortho*-nitrogen atom on the adjacent heterocycle, in line with the dipole repulsion hypothesis.



Scheme 2. Synthesis of dimers **10** (top), **11** (middle), and **12** (bottom) from terminal monomers **7** and **9**. Imidazolidin-2-one side-chains are highlighted in circles. *After 22 h an additional charge of Pd₂dba₃ (5 mol%) and Xantphos (15 mol%) was added. The reaction proceeded to completion after a further 3 h.

The conformational preferences of the corresponding oligomers were then investigated. Ureas **6** and **8** were formed according to literature methods,^[21] and used as the starting point for the iterative synthesis of oligomers (Scheme 2), with the *N*-Ph acting as a terminal inert capping group and internal standard for subsequent nOe analyses (*vide infra*). Deprotection with

thiophenol and K₂CO₃ liberated ureas **7** and **9**, and cross-coupling of the former with **3**, and the latter with **4** and **5**, afforded dimeric compounds **10**, **11** and **12** in 72%, 99% and 91% yields respectively. The conformations of all dimers^[23] were examined by single crystal X-ray diffraction (Figure 2).^[22] In all cases the urea C=O bonds are oriented *anti* to the *ortho*-nitrogen lone pair of the adjacent heteroaromatic ring. For pyrimidine **10** this has the effect that the molecule is highly curved; the monomer induces an 86° turn in the backbone, such that a helix composed of this motif would contain ~4 residues per turn. For **11** and **12**, the presence of *para*-substituted pyridazine and pyrazine linkers led to greater linearity, with monomer-induced curvatures of 154° and 139° respectively. It is likely that longer pyrazine-containing foldamers would form overall linear conformers due to the alternating disposition of the ureas (Figure 2, cartoon). The control exacted by dipole repulsion also leads to predictable positioning of the side-chains (Figure 2, right). While the distances between the C_α positions are largely unchanged across the three homo-dimers (8.1-8.7 Å), the facial projection of substituents from the plane of the foldamer is dependent on the heterocyclic linker. Thus, for the pyrimidine and pyridazine foldamers, side-chains are projected from the same face of the molecule, while the pyrazine linker leads to adjacent side-chains occupying opposite faces.

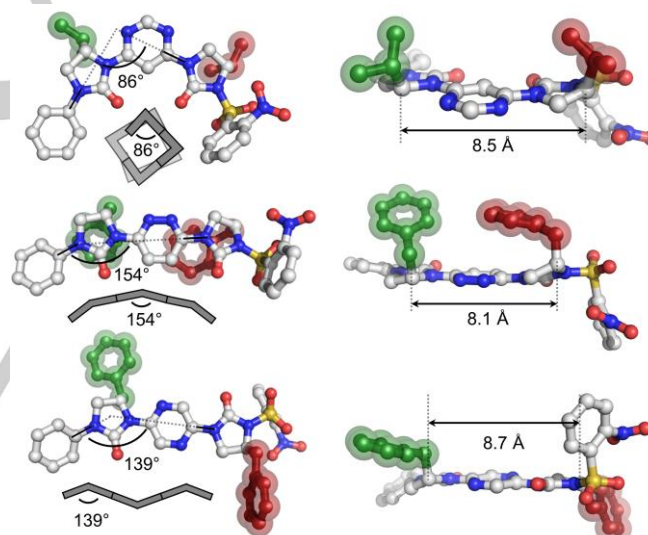


Figure 2. X-ray crystal structures of dimeric foldamers **10** (top), **11** (middle) and **12** (bottom). Left: the top elevation gives the deviation (in degrees) each monomer induces in the foldamer, where an angle of 180° would represent perfect linearity. Side-chains are highlighted in green and red. Cartoon representations of the extrapolated conformation of larger homo-oligomers are given below each structure. Right: the edge elevation shows the disposition of side-chain residues relative to the plane of the foldamer, and the distances between the C_α positions (in Å).

The solution-phase conformational behaviour of the dimers was examined through nuclear Overhauser effect (nOe) correlations. For pyrimidine **10** these indicate a strong preference towards the dipole-opposed, curved conformation (Figure 3).

COMMUNICATION

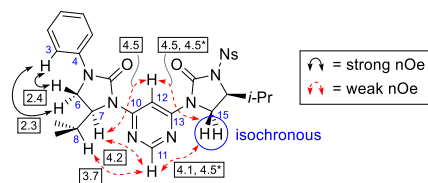


Figure 3. nOe correlations from the ROESY spectrum of **10** (CDCl_3 , 600 MHz, t_{mix} 200 ms). Solid black arrows = strong cross-peaks; dashed red arrows = weak cross-peaks. Selected atomic numbering given in blue. Numbers (in boxes) given to 1 d.p. indicate measured inter-proton distances from the X-ray crystal structure (in Å). *H15 and H11* are isochronous in the ^1H spectrum so distances for both diastereotopic hydrogens are given.

The rotating frame nuclear Overhauser effect (ROESY) cross-peaks of both H^7 and H^{15} with both H^{11} and H^{12} were of similar intensity, in agreement with the distances observed in the crystal structure. Similarly, the observed $\text{H}^8 \leftrightarrow \text{H}^{11}$ nOe indicates that the solid- and solution-phase conformations are in agreement, since these hydrogens would be too distant for an observable nOe in the alternative, dipole-*syn* conformation. In line with previous analyses,^[15e,21] the *N*-Ph group was used as an internal standard to assess conformation – it is assumed that a freely rotating *N*-C¹³ bond would lead to an observed nOe intensity ratio between $\text{H}^{12} \leftrightarrow \text{H}^{15}$ and $\text{H}^3 \leftrightarrow \text{H}^6$ of 1:2. The observed ratio was 1:25 in CDCl_3 ,^[24] indicating a strong biasing effect in solution. In 100% d_6 -DMSO at 298 K the $\text{H}^{12} \leftrightarrow \text{H}^{15}$: $\text{H}^3 \leftrightarrow \text{H}^6$ nOe ratio was 1:41, and an additional $\text{H}^3 \leftrightarrow \text{H}^{12}$ signal was observed, suggesting the molecule retains its strong preference for the dipole-opposed conformation in highly polar solvents. When warmed to 355 K the $\text{H}^{12} \leftrightarrow \text{H}^{15}$: $\text{H}^3 \leftrightarrow \text{H}^6$ nOe ratio in d_6 -DMSO fell to 1:11, suggesting a reduction in (but not loss of) conformational rigidity at elevated temperature. Analogous results (excluding d_6 -DMSO and VT experiments) were obtained for pyridazine and pyrazine dimers **11** and **12** (see supporting information).

Homo-trimers **13**, **14**, and **15**, and tetramer **16** (Figure 4) were formed by the same iterative deprotection-coupling protocol outlined in Scheme 2. Their ROESY spectra were consistent with these foldamers adopting the conformations predicted by the dipole repulsion hypothesis, with indicative couplings analogous to those in Figure 3 (see supporting information).

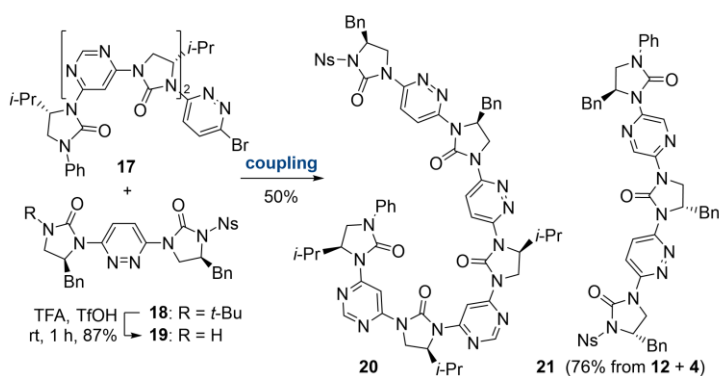


Figure 5. Left: fragment coupling approach to pyrimidine-pyridazine pentamer **20**. For coupling conditions, see Scheme 2. Middle and right: hetero-trimers **21** and **22** formed via iterative deprotection-cross-coupling. Structures are drawn in the dipole-opposed conformations. Right: structure and truncated ROESY spectrum of **22** (CDCl_3 , 600 MHz, t_{mix} 200 ms). Solid arrows indicate selected, conformationally relevant nOe correlations. Dashed arrows indicate nOe signals which were absent from the spectrum. Regions of the 2D spectrum are highlighted in white to show the relative intensity of peaks.

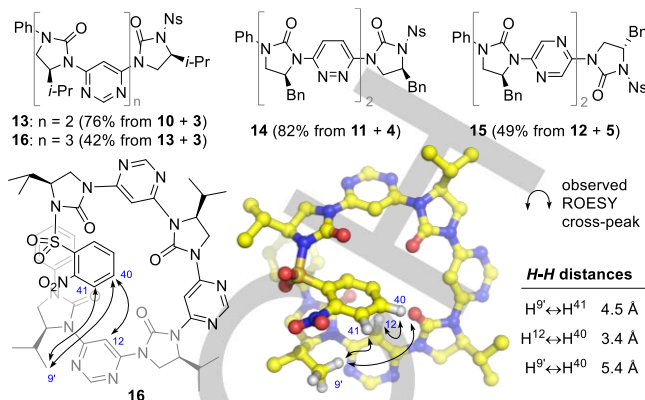


Figure 4. Top: library of homo-oligomers **13–16** synthesized through iterative cross-coupling. Bottom: arrows indicate observed long-range nOes of pyrimidine tetramer **16** (left) and its unconstrained lowest energy conformation (middle).^[25] Atom numbers are indicated in blue. The distances given (right) are from the energy-minimized structure. Where distances are measured to H^9 , the values given are an average across the three hydrogen atom positions.

Tetramer **16** gave several long-range nOe correlations (Figure 4), indicating that its ends sit in close proximity, as expected on the basis of the 86° turn per monomer outlined in Figure 2. When compared with the computed low-energy structure,^[25] these nOes correspond to close contacts in the global minimum, suggesting the (*P*)-helical conformation is significantly populated in solution. The circular dichroism spectrum of **16** displayed positive and negative Cotton effects at 300 nm and 285 nm respectively that were absent from the spectra of homologous pyrimidine dimer **10** and trimer **13**, and may be diagnostic of (*P*)-helix formation.^[26] Lastly we examined whether the conformational preferences established above were borne out in hetero-oligomers. These are expected to form structures containing distinct conformational domains, as determined by the constituent monomers. Trimers **21** and **22** were synthesized by the iterative route detailed in Scheme 2, while pentamer **20** was formed in 50% yield via a convergent strand-coupling approach from trimeric fragment **17** and dimeric **19** (Figure 5; for complete synthetic details refer to the supporting information). The solution-phase conformations of these foldamers were probed by examining their ROESY spectra.

COMMUNICATION

On the basis of the results obtained for the homo-oligomers, hetero-trimer **22** (Figure 5, right) was expected to favour a conformation curved at the pyrimidine and linear at the pyridazine linkers along its backbone. This was found to be the case, with the observation of several key nOe correlations – namely $H^3 \leftrightarrow H^{11}$, $H^7 \leftrightarrow H^{13}$, $H^8 \leftrightarrow H^{13}$ and $H^{13} \leftrightarrow H^{15}$ – indicating a strong preference for the predicted conformations about both *N*-*C*_{pyrimidine} bonds (as shown). Similarly, the absence of $H^{16} \leftrightarrow H^{20}$ and $H^{21} \leftrightarrow H^{24}$ correlations is consistent with the illustrated conformation around both *N*-*C*_{pyridazine} bonds. Foldamers **20** and **21** displayed analogous spectral features, indicating that they adopt the dipole-opposed conformations depicted in Figure 5 (see supporting information). This confirms that the design strategy described herein allows the construction of bespoke oligomers with predictable, non-repetitive conformations.

In conclusion, we have developed a chiral amino alcohol-derived foldamer backbone incorporating pyrimidine, pyridazine and pyrazine linkers, synthesized primarily through an iterative deprotection-coupling sequence. These foldamers reliably adopt conformations which can be predicted using a simple dipolar repulsion argument, even in highly polar solvents. As well as giving control of the overall backbone shape, this permits the projection of side-chains from multiple faces of the foldamer by choice of linker, enabling rapid and programmable exploration of macromolecular conformational space.

Acknowledgements

We acknowledge financial support from the Royal Society (RG160614, PCK), the EPSRC (EP/R021481/1, PCK) and Queen's University Belfast (start-up grant, PCK), and thank Professor Eric V. Anslyn for helpful discussions in the preparation of this manuscript.

Keywords: foldamers • oligomerization • conformational analysis • protein-protein interactions

- [1] C. B. Anfinsen, *Science* **1973**, *181*, 223–230.
- [2] K. A. Dill, S. B. Ozkan, M. S. Shell, T. R. Weikl, *Annu. Rev. Biophys.* **2008**, *37*, 289–316.
- [3] For reviews see: a) S. H. Gellman, *Acc. Chem. Res.* **1998**, *31*, 173–180; b) C. M. Goodman, S. Choi, S. Shandler, W. F. DeGrado, *Nat. Chem. Biol.* **2007**, *3*, 252–262; c) D. J. Hill, M. J. Mio, R. B. Prince, T. S. Hughes, J. S. Moore, *Chem. Rev.* **2001**, *101*, 3893–4011; d) S. Hecht, I. Huc, Eds., *Foldamers: Structure, Properties and Applications*, Wiley-VCH Verlag GmbH & Co. KGaA, Weinheim, Germany, **2007**; e) G. Guichard, I. Huc, *Chem. Commun.* **2011**, *47*, 5933–5941; f) D.-W. Zhang, X. Zhao, J.-L. Hou, Z.-T. Li, *Chem. Rev.* **2012**, *112*, 5271–5316; g) I. Saraogi, A. D. Hamilton, *Chem. Soc. Rev.* **2009**, *38*, 1726–1743; h) T. A. Martinek, F. Fülöp, *Chem. Soc. Rev.* **2012**, *41*, 687–702.
- [4] a) G. Maayan, M. D. Ward, K. Kirshenbaum, *Proc. Natl. Acad. Sci. U. S. A.* **2009**, *106*, 13679–13684; b) M. M. Müller, M. A. Windsor, W. C. Pomerantz, S. H. Gellman, D. Hilvert, *Angew. Chem. Int. Ed.* **2009**, *48*, 922–925; c) C. Mayer, M. M. Müller, S. H. Gellman, D. Hilvert, *Angew. Chem. Int. Ed.* **2014**, *53*, 6978–6981.
- [5] a) F. G. A. Lister, B. A. F. Le Bailly, S. J. Webb, J. Clayden, *Nat. Chem.* **2017**, *9*, 420–425; b) B. A. F. Le Bailly, J. Clayden, *Chem. Commun.* **2016**, *52*, 4852–4863.
- [6] a) O. Keskin, N. Tuncbag, A. Gursoy, *Chem. Rev.* **2016**, *116*, 4884–4909; b) G. Zinzalla, D. E. Thurston, *Future Med. Chem.* **2009**, *1*, 65–93; c) I. M. Mándity, F. Fülöp, *Expert Opin. Drug Discov.* **2015**, *10*, 1163–1177; d) J. W. Checco, S. H. Gellman, *Curr. Opin. Struct. Biol.* **2016**, *39*, 96–105.
- [7] a) J. Zhu, R. D. Parra, H. Zeng, E. Skrzypczak-Jankun, X. C. Zeng, B. Gong, *J. Am. Chem. Soc.* **2000**, *122*, 4219–4220; b) B. Gong, *Chem. Eur. J.* **2001**, *7*, 4336–4342; c) B. Gong, H. Zeng, J. Zhu, L. Yua, Y. Han, S. Cheng, M. Furukawa, R. D. Parra, A. Y. Kovalevsky, J. L. Mills, E. Skrzypczak-Jankun, S. Martinovic, R. D. Smith, C. Zheng, T. Szyperski, X. C. Zeng, *Proc. Natl. Acad. Sci. U. S. A.* **2002**, *99*, 11583–11588; d) *Curr. Org. Chem.* **2003**, *7*, 1649–1659; e) *Chem. Commun.* **2012**, *48*, 12142–12158; f) *Org. Lett.* **2017**, *19*, 2666–2669.
- [8] a) J. Garric, J.-M. Léger, I. Huc, *Angew. Chem. Int. Ed.* **2005**, *44*, 1954–1958; b) H. Jiang, J.-M. Léger, I. Huc, *J. Am. Chem. Soc.* **2003**, *125*, 3448–3449; c) for recent incorporation of foldamers into ribosomal synthesis see J. M. Rogers, S. Kwon, S. J. Dawson, P. K. Mandal, H. Suga, I. Huc, *Nature Chem.* **2018**, *10*, 405–412.
- [9] M. Burns, S. Essafi, J. R. Bame, S. P. Bull, M. P. Webster, S. Balieu, J. W. Dale, C. P. Butts, J. N. Harvey, V. K. Aggarwal, *Nature* **2014**, *513*, 183–188.
- [10] For discussion of conformational control in acyclic molecules with an emphasis on hydrocarbons, see R. W. Hoffmann, *Angew. Chem. Int. Ed.* **2000**, *39*, 2054–2070 and references therein.
- [11] M. Barboiu, A. M. Stadler, J. M. Lehn, *Angew. Chem. Int. Ed.* **2016**, *55*, 4130–4154.
- [12] a) G. S. Hanan, J.-M. Lehn, N. Kyritsakas, J. Fischer, *J. Chem. Soc. Chem. Commun.* **1995**, 765–766; b) M. Ohkita, J.-M. Lehn, G. Baum, D. Fenske, *Chem. Eur. J.* **1999**, *5*, 3471–3481; c) D. M. Bassani, J.-M. Lehn, G. Baum, D. Fenske, *Angew. Chem. Int. Ed.* **1997**, *36*, 1845–1847; d) L. A. Cuccia, J.-M. Lehn, J.-C. Homo, M. Schmutz, *Angew. Chem. Int. Ed.* **2000**, *39*, 233–237; e) L. A. Cuccia, E. Ruiz, J.-M. Lehn, J.-C. Homo, M. Schmutz, *Chem. Eur. J.* **2002**, *8*, 3448–3457.
- [13] M. S. Betson, J. Clayden, H. K. Lam, M. Helliwell, *Angew. Chem. Int. Ed.* **2005**, *44*, 1241–1244.
- [14] J. Clayden, A. Lund, L. Vallverdú, M. Helliwell, *Nature* **2004**, *431*, 966–971.
- [15] a) A. B. Smith III, A. K. Charnley, R. Hirschmann, *Acc. Chem. Res.* **2011**, *44*, 180–193; b) V. Azzarito, K. Long, N. S. Murphy, A. J. Wilson, *Nat. Chem.* **2013**, *5*, 161–173; c) S. Fahs, Y. Patil-Sen, T. J. Snape, *ChemBioChem* **2015**, *16*, 1840–1853; d) E. A. German, J. E. Ross, P. C. Knipe, M. F. Don, S. Thompson, A. D. Hamilton, *Angew. Chem. Int. Ed.* **2015**, *54*, 2649–2652; e) T. Yamashita, P. C. Knipe, N. Busschaert, S. Thompson, A. D. Hamilton, *Chem. Eur. J.* **2015**, *21*, 14699–14702.
- [16] a) R. P. Cheng, W. F. DeGrado, *J. Am. Chem. Soc.* **2002**, *124*, 11564–11565; b) J. L. Price, E. B. Hadley, J. D. Steinkruger, S. H. Gellman, *Angew. Chem. Int. Ed.* **2010**, *49*, 368–371; c) N. Delsuc, S. Massip, J.-M. Léger, B. Kauffmann, I. Huc, *J. Am. Chem. Soc.* **2011**, *133*, 3165–3172; d) J. J. L. M. Cornelissen, J. J. M. Donners, R. de Gelder, W. Sander Graswinckel, G. A. Metselaar, A. E. Rowan, N. A. J. M. Sommerdijk, R. J. M. Nolte, *Science* **2001**, *293*, 676–680; e) G. W. Collie, K. Pulka-Ziach, C. M. Lombardo, J. Fremaux, F. Rosu, M. Decossas, L. Mauraan, O. Lambert, V. Gabelica, C. D. Mackereth, G. Guichard, *Nat. Chem.* **2015**, *7*, 871–878.
- [17] a) K. L. George, W. S. Horne, *J. Am. Chem. Soc.* **2017**, *139*, 7931–7938; b) Z. E. Reinert, G. A. Lengyel, W. S. Horne, *J. Am. Chem. Soc.* **2013**, *135*, 12528–12531.
- [18] T. W. Craven, R. Bonneau, K. Kirshenbaum, *ChemBioChem* **2016**, *17*, 1824–1828.
- [19] A. Lamouroux, L. Sebaoun, B. Wicher, B. Kauffmann, Y. Ferrand, V. Maurizot, I. Huc, *J. Am. Chem. Soc.* **2017**, *139*, 14668–14675.
- [20] W. S. Horne, S. H. Gellman, *Acc. Chem. Res.* **2008**, *41*, 1399–1408.
- [21] P. C. Knipe, S. Thompson, A. D. Hamilton, *Chem. Commun.* **2016**, *52*, 6521–6524.
- [22] CCDC 1824641 (3), 1824637 (4), 1824639 (5), 1824642 (10), 1824638 (11), 1825640 (12) contain the supplementary crystallographic data for this paper. These data are provided free of charge by The Cambridge Crystallographic Data Centre.
- [23] We use the terms monomer, dimer, trimer etc. to indicate the number of imidazolidin-2-one rings present within a given molecule.
- [24] The sum of $H^3 \leftrightarrow H^6$ and $H^3 \leftrightarrow H^6$, relative to the sum of $H^{12} \leftrightarrow H^{15}$ and $H^{12} \leftrightarrow H^{15}$ cross-peak integrals.

COMMUNICATION

-
- [25] a) J. J. P. Stewart, *MOPAC 2016*, Stewart Computational Chemistry, Colorado Springs, CO (USA), **2016**; b) J. J. P. Stewart, *J. Mol. Model.* **2013**, *19*, 1–32.
- [26] CD spectra of all foldamers in this study are supplied and discussed in the supporting information.

WILEY-VCH

Accepted Manuscript

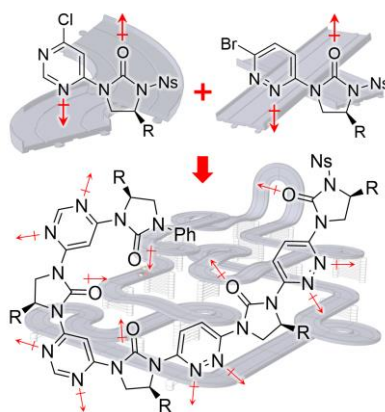
COMMUNICATION

Entry for the Table of Contents (Please choose one layout)

Layout 1:

COMMUNICATION

Know when to fold 'em: the use of isomeric heterocyclic linkers afforded a foldamer where the choice of monomer predictably controls the conformation of the macromolecule, analogous to a model car racing set constructed from individual pieces (see graphic). The conformation is enforced by a strong dipole repulsion effect, and was demonstrated using X-ray and 2D NMR techniques.



Zachariah Lockhart and Peter C. Knipe*

Page No. – Page No.

**Conformationally Programmable
Chiral Foldamers with Compact and
Extended Domains Controlled by
Monomer Structure**